An electromagnetic localization method for medical micro-devices based on adaptive particle swarm optimization with neighborhood search

Guo Xudong *, Wang Cheng, Yan Rongguo

School of Medical Instrument and Food Engineering, University of Shanghai for Science and Technology, Shanghai 200093, China

ARTICLE INFO

ABSTRACT

In order to non-invasively track a medical micro-device in gastrointestinal tract, an alternating electromagnetic tracking method was presented and a prototype was developed. In the tracking method, several energizing coils were excited by time-sharing sinusoidal signal to generate varying magnetic fields by one coil and then another coil. A wireless magnetic sensor measured the magnetic field strength at the location of the micro-device. The root-mean-square value of the magnetic field strength is a high-order nonlinear system of equations with respect to the position and orientation of the micro-device. Based on the adaptive particle swarm optimization (PSO) with neighborhood search, the position and orientation of the micro-device could be obtained. The experimental results show that the tracking method is valid and the modified algorithm succeeds in dealing with the nonlinear system of equations in localization. Comparing to the standard PSO algorithm, it does not require a good initial guess to guarantee convergence. Furthermore, it has high precision and fast convergence.

1. Introduction

In medical diagnosis and treatment, some implantable medical micro-devices, such as wireless capsule endoscopes [1,2] and gastrointestinal monitoring capsules [3,4], are widely used as a useful complementary diagnostic tool without harmful impact on patient. Nevertheless, it is hard for doctors to know the position of the capsules in the GI tract. In order to improve the effect of diagnosis, we must determine the position of the micro-devices.

Some traditional localization methods, including X-rays, ultrasound and magnetic resonance imaging, need large and expensive equipments and do not obtain the continuous track of the object. Recently, both the SMARTPILL capsule in America and the M2A capsule in Israel were localized by measuring energy of radio frequency (RF) signals. The positional precision of the method needs to be further improved [5]. In addition, a magnetic tracking method employing a permanent magnet enclosed in micro-devices was investigated [6–10]. As for the method, the tracking scope was too small and the static magnetic field generated by permanent magnets tended to be interfered with background magnetic fields.

Considering that human body has magnetic permeability practically the same as empty space, a novel electromagnetic localization method based on adaptive particle swarm optimization (PSO) with neighborhood search was presented. The magnetic field is non-invasive and thus it is safe to be used in human body. In the localization method, several exciting coils were mounted above the patient's abdomen to generate a varying electromagnetic field by individual coils alternately. We use a magnetic sensor to measure the root-mean-square value of the magnetic field strength at the location of the micro-device. The magnetic field strength is high-order nonlinear function with respect to the position and orientation of the micro-device. Thus several simultaneous equations are formed and the position and orientation of the micro-device can be computed by an optimization algorithm. The position and orientation of the micro-device could be obtained by solving the

* Corresponding author. Tel.: +86 21 55271115; fax: +86 21 55270695.
E-mail address: guoxd@usst.edu.cn (X. Guo).

inverse problem of magnetic field. To simplify the calculation, the system of equations in the localization was transformed into a nonlinear optimization problem. Then the adaptive PSO with neighborhood search was employed to resolving the optimization problem.

2. Localization system configuration

The localization system is made up of an alternating electromagnetic field generator, a wireless magnetic sensor, a wireless data recorder and a data processing system. The block diagram of the whole system is shown in Fig. 1a.

The alternating electromagnetic field generator is mounted above the abdomen of patients when they lie on the bed. It is composed of a waveform generator, a sequence-controller and eight excitation coils. The eight excitation coils are excited one-by-one in sequence with a sinusoidal signal to generate an alternating electromagnetic field. The exciting frequency in the design is 9.26 kHz.

The wireless magnetic sensor must be mounted into or onto the micro-device which needs to be tracked. It employs micro-electro-mechanical system, wireless communication and packaging techniques. The wireless magnetic sensor is sealed in a capsule shaped shell, which is made of medical polycarbonate. The shell is about 9 mm in diameter and 10 mm in length. As shown in Fig. 1b, it is made up of the following functional blocks: batteries, a power manager, an induction coil, a signal processor and radio frequency (RF) transmitter. As long as there exist available spaces inside or on the micro-device, the sensor can be fixed and move along with the micro-device. The root-mean-square values of induction electromotive forces corresponding to the eight excitation coils can be measured and then transmitted to the wireless data recorder.

The wireless data recorder, which is composed of a RF receiver and a flash memory card, is mounted around waist. The output from the magnetic sensor can be wirelessly received by the RF receiver and then saved in the memory card. All data in the memory card can be downloaded to the data processing system. By means of the localization model [11] and the particle swarm optimization algorithm, the position and orientation of the micro-devices can be finally calculated and displayed in the PC.

3. Principle of localization

As illustrated in Fig. 2, a reference coordinate system denoted by $o-xyz$ is attached to human body. The navel is taken as an origin. Z axis is perpendicular to the surface of the back and points to the body. Y axis is parallel to the spine and points to the head. Eight excitation coils are arranged on the abdomen surface of the body.

A moving coordinate system $o'-x'y'z'$ is attached to the wireless magnetic sensor. The center of the wireless magnetic sensor is denoted by o' and the central principal axis is denoted by $o'z'$. The coordinate of point o' relative to the reference coordinate system is (x, y, z). The angle between $o'z'$ and z axis is denoted by α and the angle between x axis and the projection of $o'z'$ onto $x-o-y$ plane is denoted by β. When the wireless magnetic sensor rotated around its central principal axis, its output does not change. Therefore, only three positional coordinates and the above two angles are relevant to the electrical signals output from the wireless magnetic sensor.

The excitation current is a sinusoidal signal given by $I = I_p \cdot \sin \omega t$, where I_p is the peak value of the sinusoid, ω is the angular frequency. And the radius of the excitation coil is denoted by a. n represents the total turns of the excitation coil. The central coordinate of excitation coil i is $(p_i, q_i, 0)$. At point (x, y, z), the rate of change of magnetic flux density generated by coil i is given as follows [11]:

$$\left.\begin{aligned}
\frac{dB_{ix}}{dt} &= \frac{n\mu_0 a^2 I_p \cdot \omega \cdot \cos \omega t}{4(R^2+a^2)^{3/2}} \cdot \left\{ \frac{3(x-p_i)z}{R^2+a^2} + \frac{105a^2(x-p_i)^3 z}{8(R^2+a^2)^3} \right. \\
&\left. + \frac{105a^2(x-p_i)(y-q_i)^2 z}{8(R^2+a^2)^3} \right\} \\
\frac{dB_{iy}}{dt} &= \frac{n\mu_0 a^2 I_p \cdot \omega \cdot \cos \omega t}{4(R^2+a^2)^{3/2}} \cdot \left\{ \frac{3(y-q_i)z}{R^2+a^2} + \frac{105a^2(y-q_i)^3 z}{8(R^2+a^2)^3} \right. \\
&\left. + \frac{105a^2(x-p_i)^2(y-q_i)z}{8(R^2+a^2)^3} \right\} \\
\frac{dB_{iz}}{dt} &= \frac{n\mu_0 a^2 I_p \cdot \omega \cdot \cos \omega t}{4(R^2+a^2)^{3/2}} \cdot \left\{ 2 - \frac{3((x-p_i)^2+(y-q_i)^2)}{R^2+a^2} \right. \\
&\left. + \frac{15a^2((x-p_i)^2+(y-q_i)^2)}{2(R^2+a^2)^2} - \frac{105a^2((y-q_i)^2+(x-p_i)^2)^2}{8(R^2+a^2)^3} \right\}
\end{aligned}\right\} \quad (1)$$

where $R = \sqrt{(x-p_i)^2 + (y-q_i)^2 + z^2}$, $i = 1, 2, \ldots, 8$; μ_0 is the permeability in vacuum.

Based on the Faraday law of electromagnetic induction, the wireless magnetic sensor [12] including an induction coil generates an induced electromotive force. The electromotive force generated by coil i can be derived as follows:
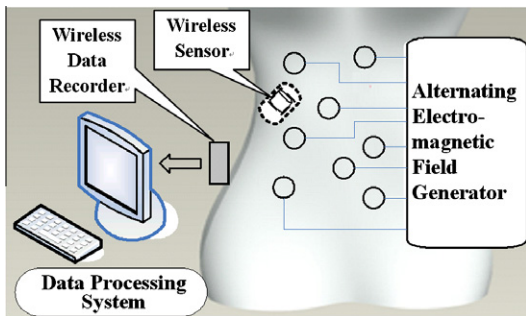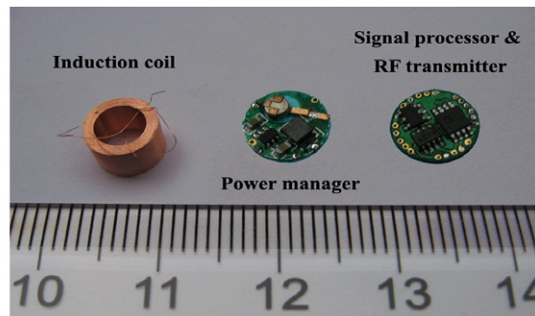
Fig. 1. Configuration of the localization system. (a) Block diagram of the localization system. (b) Modules of the magnetic sensor.
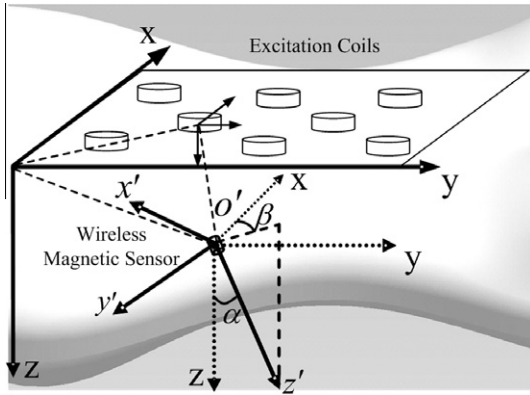
Fig. 2. Schematic diagram of the spatial position and orientation.

$$e_i = -N \cdot S \cdot [\sin\alpha \cdot \cos\beta \quad \sin\alpha \cdot \sin\beta \quad \cos\alpha] \begin{bmatrix} \frac{dB_{ix}}{dt} \\ \frac{dB_{iy}}{dt} \\ \frac{dB_{iz}}{dt} \end{bmatrix},$$
$$i = 1, 2, \ldots, 8 \tag{2}$$

where N represents the total turns of the induction coil; S represents the cross sectional area of the induction coil.

The root-mean-square values of electromotive forces generated by coil i can be further simplified as follows:

$$e_m^i = -N \cdot S \cdot [\sin\alpha \cdot \cos\beta \quad \sin\alpha \cdot \sin\beta \quad \cos\alpha] \begin{bmatrix} VB_{mx}^i \\ VB_{my}^i \\ VB_{mz}^i \end{bmatrix},$$
$$i = 1, 2, \ldots, 8 \tag{3}$$

where e_m^i is the root-mean-square values of electromotive force generated by coil i; VB_{mx}^i, VB_{my}^i and VB_{mz}^i is the root-mean-square values of dB_{ix}/dt, dB_{iy}/dt and dB_{iz}/dt, respectively.

Thus, the relation between the electromotive force and the position and orientation of the wireless magnetic sensor is finally established. Nevertheless, the system of equations with five variables is extremely complex. In order to solve it, the equation set is converted to an objective function as follows.

$$\min f(P) = \sqrt{\sum_{i=1}^{8} \{e_m^i + N \cdot S \cdot [\sin\alpha \cdot \cos\beta \quad \sin\alpha \cdot \sin\beta \quad \cos\alpha] \begin{bmatrix} VB_{mx}^i \\ VB_{my}^i \\ VB_{mz}^i \end{bmatrix}\}^2} \tag{4}$$

where $P = [x, y, z, \alpha, \beta]^T, P \in \Phi$, Φ is the interval of the solution to the equation set.

The global minima to the objective function (4) can be obtained only when the five variables equal to the solution of the equation set. The objective function has multi-variables to optimize and quite a lot of local minima, which results in difficulties in dealing with the function. Some traditional algorithms, including Newton method, steepest descent and least-square method, must require a good

initial guess to guarantee convergence. Hence the modified PSO algorithm has been introduced to solve the localization problem.

4. Adaptive particle swarm optimization with neighborhood search

4.1. The standard PSO

The PSO is a swarm intelligence method for global optimization [13]. First, let us define the notation adopted in this paper: assuming that the search space is D-dimensional, the ith particle of the swarm is represented by a D-dimensional vector $X_i = (x_{i1}, x_{i2}, x_{i3}, \ldots, x_{iD})$ and the best particle of the swarm, i.e. the particle with the smallest objective function value, is denoted by index g. The best previous position (i.e. the position giving the lowest function value) of the ith particle is recorded and represented as $P_i = (p_{i_1}, p_{i_2}, p_{i_3}, \ldots, p_{i_D})$, and the position change (i.e. velocity) of the ith particle is $V_i = (v_{i1}, v_{i2}, v_{i3}, \ldots, v_{iD})$.

The particles are manipulated according to the following equations:

$$V_i^{n+1} = \omega V_i^n + c_1 r_{i1}^n (P_i^n - X_i^n) + c_2 r_{i2}^n (P_g^n - X_i^n) \tag{5}$$

$$X_i^{n+1} = X_i^n + \chi V_i^{n+1} \tag{6}$$

where the superscripts denote the iteration; $i = 1, 2, \ldots, N, N$ is the size of the population; χ is a constriction factor which is used to control and constrict velocities; ω is the inertia weight; c_1 and c_2 are two positive constants, called the cognitive and social parameter respectively; r_{i1}^n and r_{i2}^n are two random numbers uniformly distributed within the range [0, 1].

In PSO, the problem solution space is formulated as a search space. Each particle position in the search space is a candidate solution to the problem. Particles cooperate to determine the best position in the search space.

4.2. Decaying values of parameters

In order to improve PSO's performance on the localization problem, we introduced adaptive parameters in Eq. (5), resulting in better convergence rates. And then in the final stage Powell algorithm was employed to perform neighborhood search to speed up the convergence.

In the preliminary stage, we attempted to decay the values of the inertia weight and the social parameter for the PSO algorithm. In the PSO method, each particle (or potential solution) is assigned with a random velocity and flown through the solution parameter space. Each potential solution retains the coordinates and the best fitness value associated with the best solution that particle achieved so far. This solution is referred to as PBEST (i.e. the personal best solution). The PSO algorithm also maintains the coordinates and the value of the best solution achieved by the whole population. This solution is known as GBEST (i.e. the global best solution). The particles make very large movements, thereby scanning the whole parameter space for the global minima. The inertia weight ω regulates the trade-off between the global and the local exploration

abilities of the swarm. A large inertia weight facilitates global exploration, while a small one tends to facilitate local exploration. The social parameter c_2 represents the collaborative effect of the particles, in finding the global optimal solution. The social component always pulls the particles toward the global best particle found so far.

The adaptive parameter values for PSO were changed using the following equations:

$$\omega(t) = \omega_{max} - \frac{t}{max} \times (\omega_{max} - \omega_{min}) \tag{7}$$

$$c_2(t) = c_{min} + \frac{t}{max} \times (c_{max} - c_{min}) \tag{8}$$

where max is total number of iterations, t is current iteration number.

We achieved the GBEST solutions by PSO algorithm in the early stage. Considering that PSO did not possess the ability to perform a fine grain search to improve upon the quality of the solutions as the number of generations was increased [14], Powell algorithm was then employed to perform a fine grain search in the final stage. This solution can be discovered by using Powell algorithm to inspect all GBEST solutions within a neighborhood.

4.3. Algorithmic description of modified PSO

In the localization problem, the desired optimization fitness function is defined in function (4). The steps of applying the modified PSO method in the localization problem are outlined as follows:

(1) Initialize a population of particles with random positions and velocities in the problem space.
(2) Assign the initial value to the inertia weight denoted by ω, the cognitive parameter denoted by c_1, the social parameter denoted by c_2, the desired accuracy denoted by ε_1, the maximum number of iterations denoted by max.
(3) Evaluate the fitness value of all particles. Compare particle's fitness evaluation with particle's PBEST. If current value is better than PBEST, then set PBEST value equal to the current value, and the PBEST location equal to the current location in the problem space.
(4) Compare fitness evaluation with the population's overall previous best. If current value is better than GBEST, then reset GBEST to the current particle's array index and value.
(5) Update the velocity of the particle according to the following equation:

$$V_i^{n+1} = \omega V_i^n + c_1 r_{i1}^n (P_i^n - X_i^n) + c_2 r_{i2}^n (P_g^n - X_i^n).$$

(6) A particle's velocity on each dimension is clamped to a maximum magnitude. If the velocity of the particle exceeds a positive constant value v_{max}, then the velocity is assigned to v_{max}. If the velocity of the particle is less than a constant value v_{min}, then the velocity is assigned to v_{min}.

(7) Update the position of the particle according to the following equation:

$$X_i^{n+1} = X_i^n + \chi V_i^{n+1}.$$

(8) Change the parameter values for the PSO using the following equation:
$$\omega(t) = \omega_{max} - \frac{t}{max} \times (\omega_{max} - \omega_{min}), c_2(t)$$
$$= c_{min} + \frac{t}{max} \times (c_{max} - c_{min}).$$

(9) Loop to step (3) until a stop criterion is satisfied or a prespecified number of iterations is completed. Then the GBEST position of the particles can be obtained as the initial value of Powell algorithm.
(10) Employ Powell algorithm to inspect all GBEST solutions within a neighborhood. If a stopping condition is satisfied, this solution to the localization problem can be achieved.

5. Experimental results

In order to prove the feasibility of applying the modified PSO in the localization problem, a simulation experiment was performed. Substitute a value of the position and orientation $(x_0, y_0, z_0, \alpha_0, \beta_0)$ into the localization equation defined in (3), then an electromotive force e_m^i can be calculated. Taking the electromotive force as known, we can inversely substitute the calculated data e_m^i into Eq. (4). Thus an objective function for localization is obtained with five variables (x, y, z, α, β). The objective function was solved by the standard PSO and the modified PSO algorithms, respectively.

For both algorithms, 100 different situations were calculated, starting with a population of particles with random positions and velocities in the problem space. Besides, the desired accuracy was 10^{-5}. During a preliminary experiment, we used four swarm sizes ($N = 20, 40, 60,$ and 80) to test both algorithms. Regarding the four different parameters, $N = 20$ exhibits low success rates in detecting the global minimum within the maximum number of allowed function evaluations. When the swarm's size is bigger than 40, the success rate is not yet improved and the processing time is increasing with the increasing of the swarm's size. The outcome of $N = 40$ was the best, so the value was used in all further tests.

For the standard PSO algorithm, the inertia weight ω was set equal to 0.8; $c_1 = c_2 = 2$; the maximum number of allowed function evaluations was set to 5000. For the modified PSO algorithm, the inertia weight ω was gradually decreased from 1.2 towards 0.65; the social parameter c_2 was gradually increased from 0.6 towards 1.6. In addition, the maximum number of iterations was set to 1000; v_{max} was set to 0.02 and v_{min} was set to -0.02. The performance of the modified PSO algorithm applied in localization was investigated by compare the results of the modified PSO and the standard PSO, as shown in Table 1.

For both algorithms, the average of the required number of iterations and the success rate in detecting the global minimum of the localization problem within the maximum number of iterations are reported in Table 1.

Table 1
Comparison of the performance for the standard and the modified PSO algorithm.

Algorithm	The average number of iterations	Success rate (%)
The standard PSO	1859	57.27
The modified PSO	433	100

The standard PSO did not possess the ability to perform a fine grain search to improve upon the quality of the solutions as the number of generations was increased. Instead, the modified PSO discovered reasonable quality solutions much faster than the standard PSO. The modified PSO guarantees the convergence and improves the convergence velocity. It outperformed the standard PSO, in terms of the mean number of required iterations. Moreover, the behavior of the modified PSO seems to be stable for solving the localization problem, exhibiting high success rates.

The solution found by the modified PSO for the localization problem is denoted by $(x_0', y_0', z_0', \alpha_0', \beta_0')$. The following equations were introduced to show the precision:

$$\Delta\alpha = |\alpha_0' - \alpha_0| \tag{9}$$

$$\Delta\beta = |\beta_0' - \beta_0| \tag{10}$$

$$\Delta r = (\Delta x^2 + \Delta y^2 + \Delta z^2)^{1/2} \tag{11}$$

where $\Delta\alpha$, $\Delta\beta$ is the error component of angle α, β, respectively; Δr is the resultant errors, Δx, Δy, Δz is the error component of x, y, z, $\Delta x = |x_0' - x_0|$, $\Delta y = |y_0' - y_0|$, $\Delta z = |z_0' - z_0|$.

From the experiment, we can conclude that the mean error component of x, y, z is 0.0023 m, 0.0024 m, 0.0026 m, respectively. The mean error component of angle α, β is 0.0336 rad, 0.0354 rad, respectively. The distribution of the resultant errors Δr is illustrated in Fig. 3. The resultant errors range from 0.0013 m to 0.0091 m. The mean value of the resultant errors is 0.0044 m. The experiment shows that the modified PSO algorithm succeeds in resolving the localization problem, independent of initial value.

In order to prove the validity of applying the modified PSO method in localization, the localization experiment was performed. A position and orientation measuring
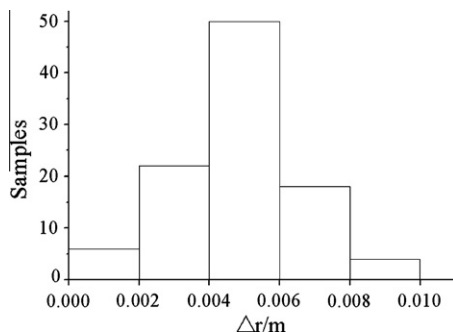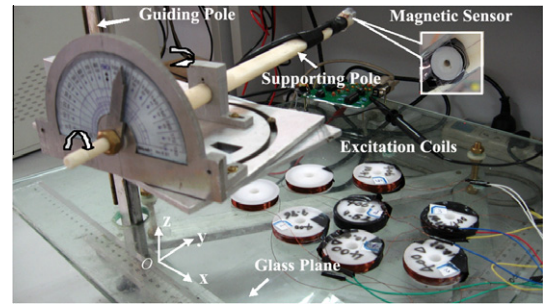

Fig. 4. The photo of the experimental apparatus.

instrument (POMI) was developed to measure the position and orientation (P&O) of the target. As shown in Fig. 4, the reference coordinate system denoted by *o-xyz* was set up in the POMI. The position of the target is described by the coordinates in the reference coordinate system and the orientation is determined based on Euler angle. The positional coordinates and attitude angles of the target could be arbitrarily adjusted and directly obtained by the indicating dials of the POMI. The adjusting steps are described as follows. Firstly, the object is movable along the guiding pole and the supporting pole. Secondly, the object can rotate around the axis of the supporting pole. Finally, the object can rotate around *z* axis as well. On glass plane of the POMI, all the excitation coils are cylinder in shape, 20 mm in diameter and 5 mm in length. The total number of turns in each coil is 400.

Arbitrarily changing the position and orientation of the magnetic sensor through the POMI, many groups of output data were recorded. Based on these data, the position and orientation were calculated by the modified PSO. In the meanwhile, the real position and orientation were directly read by means of the POMI. Comparing the calculated result with the real value, we could test the validity of the modified algorithm.

In the localization experiment, the orientation errors range from 0.0019 to 0.2302 rad. The mean error of angle component is about 0.1216 rad. The distribution of the position errors is shown in Fig. 5. The maximum error component of *x*, *y* and *z* is 0.031 m, 0.034 m, 0.029 m, respectively. The mean error component of *x*, *y* and *z* is 0.011 m, 0.014 m, 0.010 m, respectively.

In conclusion, the modified PSO is a valid method to deal with the nonlinear system of equations in localization.

The mean error components in the localization experiment are much larger than those in the simulation experiment. It is because that the errors in the simulation experiment are brought about only by the algorithm. In the algorithm the finite calculation is performed to approach to the real solution. Instead, in the localization experiment, the errors are mainly due to the localization model and the measurement instruments. The algorithm is only a minor contributor to errors, compared to the model and the instruments. In the modeling, the truncated series bring about the model error. With the decreasing of the distance *r* between the center of the magnetic sensor and the origin of the reference coordinate system, the model errors get bigger. While *r* is more than 0.3 m, the model
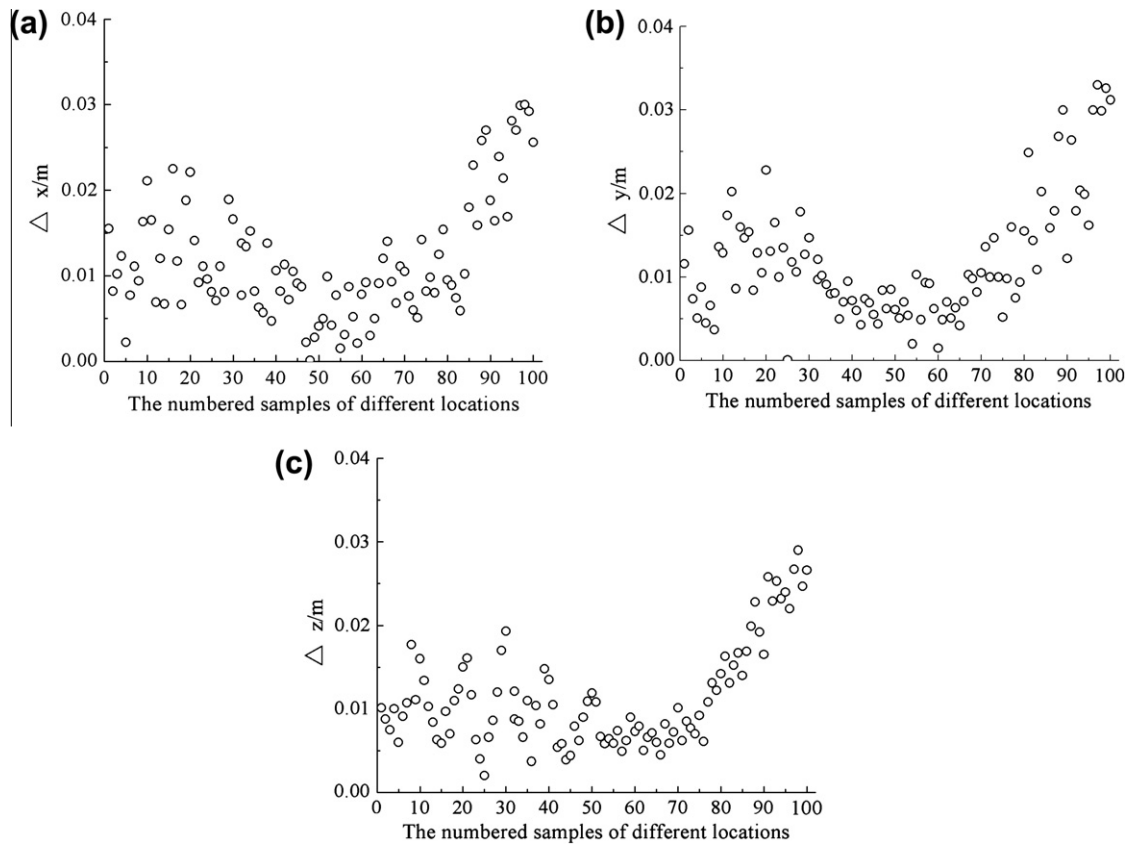

Fig. 3. Distribution of the resultant errors.

Fig. 5. Distribution of the position errors. (a) Error component of *x*. (b) Error component of *y*. (c) Error component of *z*.

Table 2
Localization errors for different porcine tissue.

Media	Error component	The number of samples		Mean error (m)
		$0 < \Delta \leqslant 0.02$ m	$0.02 < \Delta \leqslant 0.04$ m	
Meat	Δx	81	19	0.013
	Δy	83	17	0.015
	Δz	76	24	0.010
Stomach	Δx	83	17	0.012
	Δy	82	18	0.015
	Δz	75	25	0.010
Large intestine	Δx	82	18	0.014
	Δy	84	16	0.016
	Δz	76	24	0.011
Small intestine	Δx	80	20	0.013
	Δy	81	19	0.016
	Δz	74	26	0.011
Empty space	Δx	84	16	0.011
	Δy	85	15	0.014
	Δz	78	22	0.010

error is small. Meanwhile, the signal intensity received by the magnetic sensor sharply decreases, which results in a low signal-to-noise ratio. Both the noise produced by the circuit and the background interference lowered the measurement precision. In addition, the alternating magnetic field will inevitably be distorted due to the eddy currents induced in nearby metals when the field is changing. Therefore metal objects in the vicinity of excitation coils may reduce the localization accuracy.

In order to estimate the influence of body tissue, porcine body tissue including layers of meat, stomach, large intestine and small intestine from freshly killed pig was used. The layers of meat included skin, fat, muscle and rib bones, which was about 6 cm thick and weighted 5 kg. The wireless magnetic sensor was embedded in the porcine tissue. For each kind of tissue, the localization experiments were performed and the position error is analyzed in Table 2.

The experimental results show that porcine body tissue has little effect on the localization method. This is expected because porcine tissue has magnetic permeability practically the same as empty space. Thus its loss in the low frequency electromagnetic field is expected to be small.

6. Conclusions

In this paper, we investigated the performance of adaptive PSO with neighborhood search applied into the localization problem. In particular, we proposed a number of improvements including time-varying inertia weight values and the social parameter values, introducing Powell algorithm for performing a fine grain search within a neighborhood.

The experimental results show that the modified PSO is a valid method to deal with the nonlinear system of equations in localization. The standard PSO did not possess the ability to perform a fine grain search to improve upon the quality of the solutions as the number of generations was increased. Instead, the modified PSO discovered reasonable quality solutions much faster than the standard PSO. Independent of initial values, the modified algorithm displays very high success rate and improves the convergence velocity. Furthermore, it has high precision.

Acknowledgements

References

[1] G. Iddan, G. Meron, A. Glukhovsky, P. Swain, Wireless capsule endoscopy, Nature 405 (2000) 417–420.
[2] S. Neumann, K. Schoppmeyer, T. Lange, M. Wiedmann, J. Golsong, A. Tannapfel, J. Mossner, D. Niederwieser, K. Caca, Wireless capsule endoscopy for diagnosis of acute intestinal graft-versus-host disease, Gastrointestinal Endoscopy 65 (2007) 403–409.
[3] Youhong Fang, Chunxiao Chen, Bingling Zhang, Effect of small bowel preparation with simethicone on capsule endoscopy, Journal of Zhejiang University Science B 10 (2009) 46–51.
[4] Erik A. Johannessen, Lei Wang, Stuart W.J. Reid, David R.S. Cumming, Jon M. Cooper, Implementation of radiotelemetry in a lab-in-a-pill format, Lab on a Chip 6 (2006) 39–45.
[5] Harold Jacob, Daphna Levy, Reuben Shreiber, Arkady Glukhovsky, Doron Fischer, Localization of the given M2A ingestible capsule in the given diagnostic imaging system, Gastrointestinal Endoscopy 55 (2002) AB135.
[6] E. Stathopoulos, V. Schlageter, B. Meyrat, Y. Ribaupierre, P. Kucera, Magnetic pill tracking: a novel non-invasive tool for investigation of human digestive motility, Neurogastroenterol Motility 17 (2005) 148–154.
[7] Xiaona Wang, M.Q.-H. Meng, Chao Hu, A localization method using 3-axis magnetic sensors for tracking of capsule endoscope, in: Proceedings of the 28th Annual International Conference of the IEEE Engineering in Medicine and Biology Society. New York, USA, 2006, pp. 2522–2525.
[8] Wenhui He, Guozheng Yan, Xudong Guo, Capsule location detection based on magnetoresistive sensor in GI, Chinese Journal of Scientific Instrument 27 (2006) 1187–1190.
[9] Xudong Wu, Wensheng Hou, Chenglin Peng, Xiaolin Zheng, Xing Fang, Jin He, Wearable magnetic locating and tracking system for MEMS medical capsule, Sensors and Actuators A: Physical 141 (2008) 432–439.
[10] W. Weitschies, H. Blume, H. Mönnikes, Magnetic marker monitoring: high resolution real-time tracking of oral solid dosage forms in the gastrointestinal tract, European Journal of Pharmaceutics and Biopharmaceutics 74 (2010) 93–101.
[11] Xudong Guo, Guozheng Yan, Wenhui He, A position telemetric method for implantable microcapsules in the gastrointestinal tract, Measurement Science and Technology 19 (2008) 045201–045208.
[12] Xudong Guo, Guozheng Yan, Wenhui He, Design of the magnetic sensor in alternating electromagnetic localization system, Chinese Journal of Scientific Instrument 28 (2007) 1211–1216.
[13] K.E. Parsopoulos, M.N. Vrahatis, Recent approaches to global optimization problems through particle swarm optimization, Natural Computing 1 (2002) 235–306.
[14] P Angeline, Evolutionary optimisation versus particle swarm optimization: philosophy and performance difference, in: Proceedings of Evolutionary Programming Conference, San Diago, USA; 1998.